American Mineralogist, Volume 90, pages 510–515, 2005

LETTER

Ferrous hydroxy carbonate is a stable transformation product of biogenic magnetite

RAVI K. KUKKADAPU,* JOHN M. ZACHARA, JAMES K. FREDRICKSON, DAVID W. KENNEDY, ALICE C. DOHNALKOVA, AND DAVID E. MCCREADY

Pacific Northwest National Laboratory, Richland, Washington 99352, U.S.A.

ABSTRACT

An ~1:1 mixture of ferrihydrite and nanocrystalline akaganeite (β-FeOOH; 10–15 nm) was incubated with *Shewanella putrefaciens* (strain CN32) under anoxic conditions with lactate as an electron donor and anthraquinone-2,6-disulfonate (AQDS) as an electron shuttle. The incubation was carried out in a 1,4-piperazinediethanesulfonic acid (PIPES)-buffered medium, without PO_4^{3-} at circumneutral pH. Iron reduction was measured as a function of time (as determined by 0.5 N HCl extraction), and solids were characterized by X-ray diffraction (XRD), electron microscopy, and Mössbauer spectroscopy. The biogenic reduction of $Fe^{3+}$was rapid; with 60% of the total Fe (Fe_{TOT}) reduced in one day. Only an additional 10% of Fe_{TOT} was reduced over the next three years. A fine-grained (~10 nm), cation-excess (CE) magnetite with an Fe^{2+}/Fe_{TOT} ratio of 0.5–0.6 was the sole biogenic product after one day of incubation. The CE magnetite was unstable and partially transformed to micrometer-sized ferrous hydroxy carbonate [FHC; $Fe_2(OH)_2CO_{3(s)}$], a rosasite-type mineral, with time. Ferrous hydroxy carbonate dominated the mineral composition of the three year incubated sample. The Fe^{2+}/Fe_{TOT} ratio of the residual CE magnetite after three years of incubation was lower than the day 1 sample and was close to that of the stoichiometric magnetite (0.33). To the best of our knowledge, this is the first report of biogenic FHC, and was only reported twice in literature but in a very different context. Ferrous hydroxy carbonate appeared to form by slow reaction of microbially produced carbonate with Fe^{2+}-excess magnetite. The FHC may be an overlooked mineral phase that explains the infrequent occurrence of fine-grained, biogenic magnetite in anoxic sediments.

INTRODUCTION

Dissimilatory Fe^{3+}-reducing bacteria (DIRB) catalyze the reduction of Fe^{3+} to Fe^{2+} in soils, sediments, and subsurface materials (Lovley 1993). These organisms utilize Fe^{3+} oxides and other Fe^{3+}-containing minerals as electron acceptors for respiration (Nealson and Little 1997) and transform them to other mineral phases that are reactive with inorganic and organic solutes. Poorly crystalline Fe^{3+}-oxides, including ferrihydrite (Jambor and Dutrizac 1998) and nanogoethite (van der Zee et al. 2003), are the most bioavailable Fe^{3+} solid-phase for DIRB. A variety of biomineralization products result from the interaction of DIRB with Fe^{3+} oxides, including magnetite, green rust (GR), vivianite, and siderite under specific conditions (Fredrickson et al. 1998). Biogenic Fe^{2+} flux rate, the presence of sorbed/coprecipitated ions, medium composition, electron donor and acceptor concentrations, crystallinity and type of Fe^{3+}-oxide are all important factors influencing the nature of biomineralization products (Zachara et al. 2002; Kukkadapu et al. 2004).

Although magnetite is a commonly observed laboratory transformation product of Fe^{3+} oxides by DIRB, there are few reports of biogenic, fine-grained magnetite in soils, sediments, and subsurface materials that have experienced in-situ dissimilatory Fe reduction (Gibbs-Eggar et al. 1999). The reasons for this absence of fine-grained magnetite in natural settings are unknown. Could magnetite be unstable under Fe-reducing conditions due to small size or other properties resulting from biosynthesis? Recently, we noted that the Fe^{2+}/Fe_{TOT} ratio of a fine-grained (10 nm), biogenic magnetite produced by DIRB (Kukkadapu et al. 2004), was in excess (0.5–0.6) of stoichiometric magnetite (0.33; e.g., Greenwood and Gibb 1979) and intracellular magnetite produced by magnetotactic bacteria (Sparks et al. 1990). Biogenic, intracellular magnetites are larger than those produced by DIRB (40–50 nm); they are stoichiometric and single domain in nature, and are more stable as they persist for long periods as microfossils in certain environments (Chang et al. 1987; Vali et al. 1987; Sparks et al. 1990).

Fe^{2+}-excess magnetites [termed as hyper-, or cation-excess (CE) magnetite], of varying Fe^{2+}/Fe_{TOT} ratio (0.4–0.6) have been reported in the materials/catalysis research areas (e.g., McCammon et al. 1986; Tamaura and Tahata 1990; Tamaura et al. 1994). Cation-excess magnetites are strong reductants and promote the complete reduction of carbon dioxide to carbon (Tamura and Tahata 1990). Allen et al. (2001) recently speculated that CE magnetites are important in nature, playing a significant role in carbon reduction in marine geothermal systems where magnetite formation is rapid.

The high reactivity of CE magnetite for oxidized carbon compounds compared to stoichiometric magnetite and its lack

* Present address: Pacific Northwest National Laboratory, MSIN K8-96, P.O. Box 999, Richland, Washington 99352, U.S.A. E-mail: ravi.kukkadapu@pnl.gov

0003-004X/05/0203–510$05.00/DOI: 10.2138/am.2005.1727

of persistence in soil and sediment environments where dissimilatory Fe^{3+} reduction has occurred may result from its excess Fe^{2+} content and small particle size. In this communication, we report the rapid production of CE magnetite from the bioreduction of a poorly crystalline Fe^{3+} oxide mixture at circumneutral pH by a single culture DIRB (*Shewanella putrefaciens*). We then followed the stability of this phase in the presence of microbial oxidation products of lactate (carbonate and acetate). Our specific objectives were to identify whether changes in the Fe^{2+}/Fe_{TOT} ratio of the biogenic CE magnetite would occur upon aging, and whether CE magnetite would exhibit instability and transform to other mineral phases. CE magnetite was found to be unstable in our experimental system and transformed to another poorly known crystalline Fe^{2+} phase. Our findings provide new insights on the long-term stability of DIRB-produced magnetite, and partially explain why this specific biosynthetic phase is infrequently observed in anoxic environments.

Materials and methods

Starting material

A ferrihydrite and akaganeite (β-FeOOH) coprecipitate was prepared by titrating a solution of $FeCl_3.6H_2O$ (0.4 mM) with 5 mM NaOH. The pH of the suspension was increased by slow, sustained addition of NaOH. After the addition of NaOH, the suspension pH was approximately 5. The suspension was stirred overnight. The pH of the suspension was brought to 7 the next day, and the mineral suspension was washed and centrifuged several times with deionized water to remove chloride. The washed suspension was stored at room temperature (RT). A subsample was dissolved in HCl and analyzed for Fe by inductively coupled plasma (ICP) spectroscopy.

Bacteria, media, and bioreduction experiments

Anoxic suspensions of *S. putrefaciens* strain CN32 were prepared and suspended in 30 mM PIPES buffered-medium (pH 7) as reported previously (Fredrickson et al. 2001). The minimal media included: lactate (27 mM) as the electron donor, and anthraquinone disulfonate (AQDS) at 0.1 mM. AQDS is a quinone that simulates the biologic reduction of Fe^{3+} oxides in a manner similar to that of humic substances (Lovley et al. 1996; Scott et al. 1998). The medium did not contain PO_4^{3-} and was not growth supporting. The Fe^{3+}-oxide mixture [at 42 mM–Fe^{3+}] was incubated with strain CN32 in PIPES buffered medium (30 mM) containing 2–4 × 10^8 cells/mL. The headspace atmosphere of the tubes was O_2-free N_2. The sealed tubes were incubated in the dark at 30 °C until sampled (up to 28 months). Each treatment and sampling event was replicated three times, and separate tubes were sacrificed at each time-point for analyses. Abiotic control samples were established at each time point. DIRB were absent in the controls, but were otherwise identical to the biotic samples.

The concentrations of Fe in aqueous filtrates (0.2 μm) and 0.5 N HCl extracts (1 hour, agitated at 25 rpm) were measured by ICP-atomic emission spectroscopy and Fe^{2+} was measured by the ferrozine assay (Stookey 1970).

Powder X-ray diffraction (XRD), Mössbauer, and electron microscopy

Powder XRD patterns were obtained with a Philips PW3040/00 X'pert MPD system, using CuK_α radiation with a variable divergent silt and solid-state detector. Mineral residues were filtered through a 0.2 μm nylon filter and washed with 1–2 mL of anoxic acetone to obtain "dry" powder samples. The powders were tightly packed into the walls (0.25 inch i.d. and 0.03 inch deep) of low-background quartz slides (Gem Dugout, Inc., Pittsburgh). Filtration, washing, and packing of the samples were carried out in an anoxic chamber whereas the measurements were performed in ambient atmosphere. The mineralogy of the solid residue was monitored (also by Mössbauer and electron microscopy) periodically with incubation time up to 28 months.

Randomly oriented absorbers were prepared for Mössbauer spectroscopy by mixing approximately 30–40 mg of the "acetone-dried" sample with petroleum jelly in 0.375 inch thick and 0.5 inch i.d. Cu holder sealed at one end with scotch tape. The holder was entirely filled with the sample mixture and sealed at the other end with scotch tape. An oxygen impermeable polymer (aluminized Mylar) was added as an outer seal on both the ends of the holder. Both the tape and polymer were snapped into the holder with rings made of carbonized-polyethyletherketone (PEEK) polymer to ensure tightness. The sample holders were stored in an anoxic chamber until analysis.

Mössbauer spectra were collected at RT and liquid nitrogen temperature (77 K) using a 50 mCi (initial strength) ^{57}Co/Rh source. The velocity transducer MVT-1000 (WissEL, Germany) was operated in constant acceleration mode (23 Hz, ±12 mm/s). Data were acquired on 1024 channels and folded to 512 channels (*Recoil* Program, University of Ottawa) to give a flat background and a zero-valent position corresponding to the center shift of a 20 μm thick α-Fe(m) foil. The transmitted radiation was recorded with an Ar-Kr proportional counter. A top loading Janis exchange gas cryostat was used to cool the samples. The source and drive assembly were held at RT for the 77 K measurements.

A drop of dilute sonicated Fe-oxide mineral suspension was applied directly to a 200-mesh copper grid coated with carbon-sputtered formvar support film, and allowed to dry anaerobically for transmission electron microscopy (TEM) analysis. Samples were examined at 200 kV with a JEOL 2010 high-resolution TEM coupled with an Oxford energy dispersive spectroscopy (EDS) system. Images were collected digitally, and analyzed with Gatan Digital Micrograph software. Samples for scanning electron microscopy (SEM) were prepared by anaerobic drying of mineral suspension aliquots applied to a carbon tape. Imaging and EDS analyses were performed using a LEO82 field emission SEM operating at 3 kV fitted with backscattered and secondary electron detectors, coupled with an Oxford EDS system.

Results and discussion

The presence of ferrihydrite and akaganeite in the initial Fe^{3+} oxide mixture was clearly evident by XRD, Mössbauer spectroscopy, and TEM (Fig. 1). The asymmetric sextet in the Mössbauer spectrum (Fig. 1b) is characteristic of akaganeite Fe^{3+} (Murad 1979). The apparent doublet (0.1 to 1 mm/s) or "collapsed" sextet feature in the spectrum, on the other hand, represents ferrihydrite (2-line/6-line; Kukkadapu et al. 2003). The akaganeite is clearly evident in TEM as 10–25 nm long rods (Fig. 1c).

CN32 rapidly oxidized lactate to bicarbonate and acetate and transferred electron equivalents to the Fe^{3+}-oxides. After 1 day, analyses of the aqueous phase and the mineral residue displayed the presence of 7.0 mM $Fe^{2+}_{(aq)}$, and 19 mM of Fe^{2+} associated with the solid phase [hereafter termed Fe^{2+}_s]. These concentrations changed slightly with further incubation: $Fe^{2+}_{(aq)}$ = 5.5 mM and Fe^{2+}_s = 24 mM after 29 days, while $Fe^{2+}_{(aq)}$ = 4.9 mM and Fe^{2+}_s = 26.1 mM after 22 months. An estimated 6.5 mM of bicarbonate (and acetate) was produced after 1 day and 7.7 mM after 22 months given the observed HCO_3^-/Fe^{2+} stoichiometry of the reaction (Fredrickson et al. 1998).

In the first day of incubation, the Fe^{3+}-oxides were transformed to fine-grained magnetite (Figs. 2a, 3a, 4a) exhibiting ~10 nm domain size, based on TEM (not shown). Nanometer-sized magnetite with globular morphology is a commonly observed laboratory product of Fe^{3+}-oxide bioreduction by DIRB in both static and advective systems (Lovley et al. 1987; Sparks et al. 1990; Zachara et al. 2002; Hansel et al. 2003; Roh et al. 2003), but such materials have been rarely identified in the field (Gibbs-Eggar et al. 1999). XRD, Mössbauer spectroscopy, and SEM showed no evidence for ferrihydrite and akaganeite, or any other phase in the mineral residue (Figs. 2a, 3a, 4a). Magnetite persisted without apparent change for an additional 7 days of incubation (Fig. 3b). Acid extraction of the 1–8 day mineral residues displayed an Fe^{2+}/Fe_{TOT} ratio (0.54–0.62) that exceeded stoichiometric magnetite (0.33; Greenwood and Gibb 1971), but was similar to that of cation excess (CE) magnetites (Fe^{2+}/Fe_{TOT}

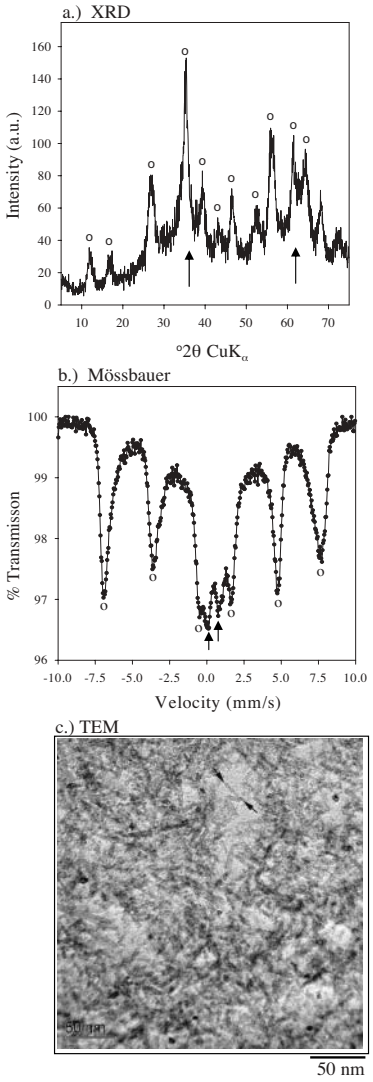

FIGURE 1. Characteristics of the ferrihydrite-akaganeite mixture. **(a)** X-ray diffractogram showing peaks due to akaganeite and ferrihydrite. Akaganeite peaks are labeled by o in the XRD pattern (PDF 34-1266), whereas the two broad peaks (25–70 °2θ) in the pattern due to ferrihydrite are indicated by arrows. **(b)** 77 K Mössbauer spectrum showing peaks due to akaganeite (asymmetric sextet component; labeled by o) and ferrihydrite (doublet or "collapsed" sextet component, indicated by arrows). Data points are connected as a guide to eye. **(c)** TEM image of an akaganeite-rich region showing crystals that are 10 to 25 nm long (indicated by arrows).

≈ 0.39–0.56; McCammon et al. 1986; Tamaura and Tahata 1990; Tamaura et al. 1994). XRD measurements of the residue showed no significant *d*-spacing differences from stoichiometric magnetite, but lattice constants of CE magnetite change only slightly with excess Fe^{2+} substitution (Tamaura and Tahata 1990; Tamaura et al. 1994). Under the assumption of stoichiometric magnetite, the chemical extraction data indicated the presence of sorbed Fe^{2+} on magnetite at a concentration of 6 mmol Fe^{2+}/g of magnetite. This rather high value represented approximately 57% of total Fe^{2+}.

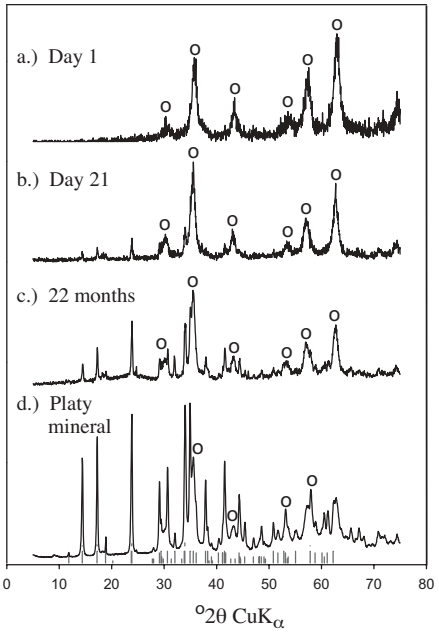

FIGURE 2. X-ray diffractograms of mineral residues resulting from the incubation of ferrihydrite-akaganeite with *Shewanella putrefaciens* CN32. **(a)** after 1 day, diffraction peaks from CE magnetite only. **(b)** after 21 days. **(c)** after 22 months. **(d)** platy mineral isolated from c; the reported diffraction peaks for ferrous hydroxy carbonate (FHC) are noted below the diffraction trace (PDF 33-0650). Magnetite peaks are labeled by o in all panels.

CE magnetite showed change after 21–28 days of incubation. New diffraction peaks were observed at 21 days (between 15–35 °2θ, Fig. 2b), a large central doublet consistent with an Fe^{2+} mineral phase was observed in the Mössbauer spectrum at 28 days (Fig. 3c), and micrometer-sized platy crystallites became visible (Fig. 4b). The crystallites grew at the expense of CE magnetite (Figs. 4b, 4c) with increasing incubation time. Concurrently, residual CE magnetite increased in its particle/aggregate size (Fig. 4c). After 22 months, the mineral residue was dominated by the platy crystallites (Fig. 4c). These exhibited a morphology (Figs. 4b, 4c) and a diffraction pattern (Fig. 2d) that matched exactly with ferrous hydroxy carbonate [FHC, $Fe_2(OH)_2CO_{3(s)}$; Erdös and Altorfer 1976]. The FHC Mössbauer doublet at 0.2–2.2 mm/s (Fig. 3c, 3d) displayed spectral parameters (center shift = 1.16 mm/s and quadrupole splitting = 1.96 mm/s) that were slightly different from siderite (Greenwood and Gibb 1971). Siderite, however, was not observed by XRD in any of the mineral residues (Fig. 2).

FHC has only been reported twice previously. In one account, it was found as the dominant mineral component (along with magnetite and siderite) of a corrosion scale on steel that formed between pH 9–11 at 180 °C and elevated pressure (Erdös and Altorfer 1976). Epitaxial relationships were observed between FHC and siderite. In another account, FHC was observed along with magnetite as reaction products in an Fe° permeable reactive barrier in contact with pH 6–7 groundwater (Wilkin and Puls 2003). FHC is a rosasite-type, basic carbonate; this mineral

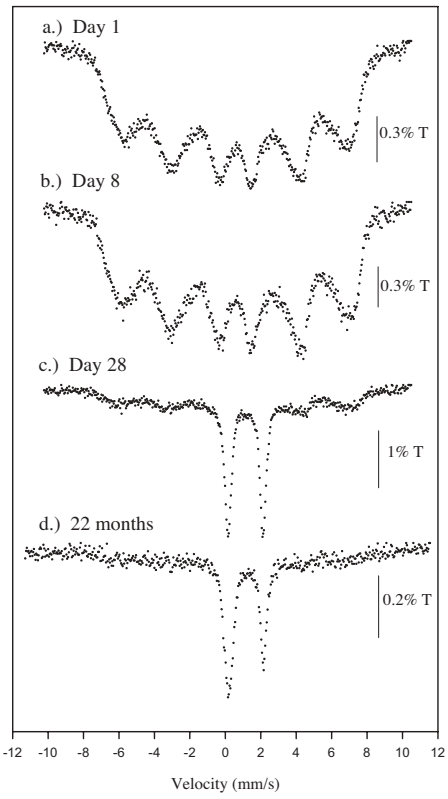

FIGURE 3. Room temperature, transmission Mössbauer spectra of incubated mineral residues (T = percent of transmission). **(a)** after 1 day, collapsed sextet resulting from fine-grained CE magnetite. **(b)** after 8 days, fine-grained CE magnetite. **(c)** after 28 days, collapsed sextet from CE magnetite and doublet from ferrous hydroxy carbonate (FHC). **(d)** after 22 months, FHC, paramagnetic Fe^{3+}, and residual CE magnetite.

class includes the well-known phase malachite [$Cu_2(OH)_2CO_3$]. The conditions of our experiments contrasted markedly with these only other reports of FHC formation that both involved the oxidation of metallic Fe.

Consistent with electron microscopy and XRD, modeling of the Mössbauer spectra showed a progressive change in CE magnetite content beginning with 100% at days 1 and 8, and decreasing to 35–40% after 22 months. In turn, the FHC content increased from 0% at day 8 to 40–45% after 22 months. The computed mass content of FHC derived from the Mössbauer spectrum at 22 months (e.g., ~45% of Fe_{TOT}, or 15.4 mM) was the maximum allowable from the carbonate produced by lactate oxidation (7.7 mM). The FHC appeared to form directly from the Fe^{2+}-enriched magnetite nanoparticles that coalesced along growth faces (center edge in Fig. 4b). Reaction with bicarbonate and recystallization to eliminate Fe^{3+}, or to enrich it in the residual CE magnetite, apparently lead to the FHC structure. Faint striations with dimensions similar to the magnetite particles were observed normal to the growth face, possibly indicating growth by nanoparticle incorporation. The CE magnetite appeared to be a key reactant in the formation of FHC.

Magnetite or siderite are the most stable Fe^{2+} containing phases between pH = 6– 10 under low Eh conditions (Benali et al. 2001). Redox measurements (Eh) on DIRB/ferrihydrite systems analogous to this one at pH ≈ 7 were near –0.35 V (Zachara et al. 2002). Here we observed that FHC was more stable than CE magnetite and siderite, although the absence of thermodynamic data for CE magnetite and FHC prevented quantitative evaluation. It is equally possible that FHC was a metastable phase. However, we have previously observed siderite formation from ferrihydrite in bicarbonate buffer containing AQDS and lactate (Fredrickson et al. 1998), and cell cytosol (Y. Gorby unpublished research) suggesting that residual organic components, metabolites, or cell debris do not inhibit siderite formation. These organic components may encourage FHC precipitation. Magnetite dissolution and remineralization in marine sediments is facilitated by organic matter and biologic metabolites (Leslie et al. 1990; Hilgenfeldt 2000).

The apparent fate of residual Fe^{3+} (16–18 mM) was difficult to assess during FHC formation. Bacterial reduction slowed after 1 day with the formation of CE magnetite that sequestered residual Fe^{3+} in an inverse spinel structure that made further reduction kinetically and thermodynamically less feasible (Kostka and Nealson 1995). Structural considerations, however, mandated that Fe^{3+} be liberated during FHC formation. Combined Mössbauer and chemical measurements indicated a general decrease in the Fe^{2+}/Fe_{TOT} ratio of the residual magnetite (to ≈ 0.45) during the initial stages of FHC formation (21–28 day), implying recrystallization of a portion of the CE magnetite. At 22 months, the formation of a distinct paramagnetic Fe^{3+} phase was implied by the increase in the low-field peak of the central doublet at 0.2 mm/s with a spectral area representing approximately 15% of Fe_{TOT} (Fig. 2d). An Fe^{3+} analog of FHC has been reported [$Fe(CO_3)OH$; Yapp 1996, 2004], but we are uncertain whether it could form here.

Although the current results were from one experimental series with a ferrihydrite/akaganeite mixture, we have observed FHC in mineral residues from multiple past experiments. Ferrihydrite (with and without coprecipitated Si) that was incubated with CN32 under identical media and buffer conditions to those used here, both with and without AQDS, showed the presence of FHC after one year of aging. Only magnetite was present in these samples when originally analyzed. Apparently, the kinetics of FHC formation can be slow, and active respiring DIRB are not necessarily required. Common to all observed occurrences of FHC were circumneutral pH with PIPES buffer and Eh <–0.20 V; CE magnetite as the initial biotransformation product; and spent media containing cells, residual lactate, and lactate oxidation products (acetate and carbonate). In all cases, FHC was observed in association with CE magnetite in an approximate 1:1 ratio. This phase ratio was regulated by the biogenic CO_3^{2-} concentration that aqueous analyses showed was almost fully incorporated into the FHC.

Our findings indicate that FHC can result from the remineralization of fine-grained, biogenic CE magnetite from DIRB under anoxic conditions. Other workers should be alert to the possible formation of FHC as an early diagenetic product of the biomagnetic mineral fraction. The apparent susceptibility of fine-grained, biogenic CE magnetite to transform to FHC may explain why the former phase is not more commonly observed in sediments that have experienced dissimilatory microbial

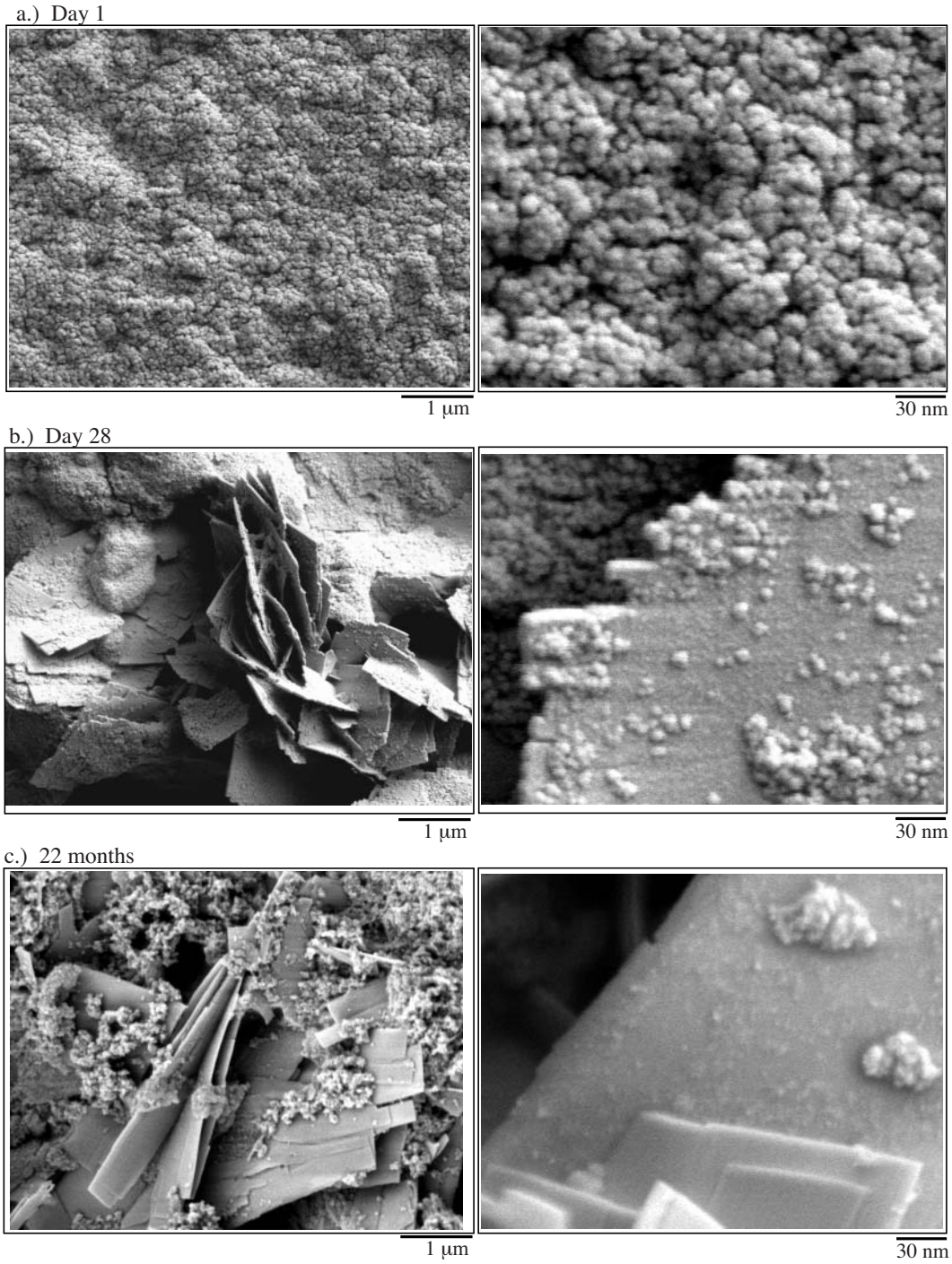

FIGURE 4. Electron micrographs of incubated mineral residues at different magnification levels. **(a)** micrographs of day 1 CE magnetite. **(b)** micrographs of the 28 day mineral residue where the left panel shows, CE magnetite as the fine-grained continuous groundmass and ferrous hydroxy carbonate (FHC) as the platy crystallites and the right panel shows a growth face on FHC. **(c)** micrographs of the 22 month mineral residue dominated by FHC.

Fe^{3+} reduction. Whether biogenic CE magnetite instability is promoted by its small, nanometer crystallite size, structural disorder, or a biosynthetic cation excess remains undetermined, although presumptive evidence suggests that cation excess is important. The conditions leading to biogenic, CE magnetite formation are unknown, as is the question of whether stoichiometric, fine-grained magnetites produced by DIRB (if any) are also unstable to FHC. CE magnetites are likely, however, to be a unique product of topotactic magnetite formation by DIRB, and possibly by post-formation reductive pressure (Kostka and Neal-

son 1995). Single-domain magnetite microcrystallites resulting from magnetotactic bacteria (Bazylinski et al. 1988; Moskowitz et al. 1989; Sparks et al. 1990), in contrast, are larger (40–50 nm), stoichiometric in composition, and appear more stable as they can persist for long periods as microfossils (Chang et al. 1987; Vali et al. 1987; Bloemendal et al. 1992).

The apparent instability of CE magnetite to FHC has important implications to magnetic stratigraphy, as our results show that a certain sequence of microbially mediated reactions may rapidly transform fine-grained magnetite from DIRB to a non-magnetic Fe^{2+} compound. Failure to recognize such transformation could lead to erroneous interpretation of the nature and timing of magnetic events as implied by magnetostratigraphy (Bloemendal et al. 1992). Furthermore, FHC will influence the reactivity of biogenic Fe^{2+} to inorganic and organic solutes as we observed that FHC was only slowly reactive with molecular oxygen.

ACKNOWLEDGMENTS

This research was supported by the Chemical Sciences Division (Geosciences Program), Basic Energy Sciences (BES), U.S. Department of Energy (DOE). Mössbauer, X-ray diffraction, and electron microscopic analyses were performed at the W.R. Wiley Environmental and Molecular Sciences Laboratory, a national scientific user facility sponsored by the U.S. Department of Energy's Office of Biological and Environmental Research and located at the Pacific Northwest National Laboratory. PNNL is operated for the Department of Energy by Battelle.

REFERENCES CITED

Allen, D.E., Hoirta, J., and Seyfried Jr., W.E. (2001) Experimental synthesis of some reduced carbon compounds: Implications for mid-ocean ridge hydrothermal systems. Eleventh Annual V.M. Goldschmidt Conference, abstract 3656.

Bazylinski, D.A., Frankel, R.B., and Jannasch, H.W. (1988) Anaerobic magnetite production by a marine, magnetotactic bacterium. Nature, 334, 518–519.

Benali, O., Abdelmoula, M., Refait, P., and Genin, J.-M.R. (2001) Effect of orthophosphate on the oxidation products of Fe^{2+}-Fe^{3+} hydroxycarbonate: The transformation of GR to ferrihydrite. Geochimica et Cosmochimica Acta, 65, 1715.

Bloemendal, J., King, J.W., Hall, F.R., and Doh, S.-J. (1992) Rock magnetism of late neogene and pleistocene deep sea sediments: Relationship to sediment source diagenetic processes, and sediment lithology. Journal of Geophysical Research, 97, 4361–4375.

Chang, S.-B.R., Stolz, J.F., and Kirschvink, J.L. (1987) Biogenic magnetite as primary reminance carrier in limestone deposits. Physics of the Earth and Planetary Interiors, 46, 289–303.

Erdös, V.E. and Altorfer, H. (1976) Ein dem Malachit ähnliches basisches Eisenkarbonat als Korrosionsprodukt von Stahl. Werkstoffe und Korrosion, 27, 304–312.

Fredrickson, J.K., Zachara, J.M., Kennedy, D.W., Onstott, T.C., Hinman, N.W., and Li, S. (1998) Biogenic iron mineralization accompanying the dissimilatory reduction of hydrous ferric oxide by a groundwater bacterium. Geochimica et Cosmochimica Acta, 62, 3239–3257.

Fredrickson, J.K., Zachara, J.M., Kukkadapu, R.K., Gorby, Y.A., Smith, S.C., and Brown, C.F. (2001) Biotransformation of Ni-substituted hydrous ferric oxide by an Fe^{3+}-reducing bacterium. Environmental Science and Technology, 35, 703–712.

Gibbs-Eggar, Z., Jude, B., Dominik, J., Loizeau, J.-L., and Oldfield, F. (1999) Possible evidence for dissimilatory bacterial magnetite dominating the magnetic properties of recent lake sediments. Earth and Planetary Science Letters, 168, 1–6.

Greenwood, N.N. and Gibb, T.C. (1971) Mössbauer Spectroscopy. Chapman and Hall, London.

Hansel, C.M., Benner, S.G., Neiss, J., Dohnalkova, A.C., Kukkadapu, R.K., and Fendorf, S. (2003) Secondary mineralization pathways induced by dissimilatory iron reduction of ferrihydrite under advective flow. Geochimica et Cosmochimica Acta, 67, 2977.

Hilgenfeldt, K. (2000) Diagenetic dissolution of biogenic magnetite in surface sediments of the Benguela upwelling system. International Journal of Earth Sciences, 88, 630.

Jambor, J.L. and Dutrizac, J.E. (1998) Occurrence and constitution of natural and synthetic ferrihydrite, a widespread iron oxyhydroxide. Chemical Reviews, 98, 2549.

Kostka, J.E. and Nealson, K.H. (1995) Dissolution and reduction of magnetite by bacteria. Environmental Science and Technology, 29, 2535–2540.

Kukkadapu, R.K., Zachara, J.M., Fredrickson, J.K., Smith, S.C., Dohnalkova, A.C., and Russell, C.K. (2003) Transformation of 2-line ferrihydrite to 6-line ferrihydrite under oxic and anoxic conditions. American Mineralogist, 88, 1903–1914.

Kukkadapu, R.K., Zachara, J.M., Fredrickson, J.K., and Kennedy, D.W. (2004) Biotransformation of 2-line silica-ferrihydrite by a dissimilatory Fe^{2+}-reducing bacterium: Formation of carbonate green rust in the presence of phosphate. Geochimica et Cosmochimica Acta, 68, 2799–2814.

Leslie, B.W., Hammond, D.E., Berelson, W.M., and Lund, S.P. (1990) Diagenesis in anoxic sediments from the California borderland and its influence on iron, sulfur, and magnetite behavior. Journal of Geophysical Research-Solid Earth and Planets, 95, 4453.

Lovley, D.R. (1993) Dissimilatory metal reduction. Annual Review of Microbiology, 47, 263–290.

Lovley, D.R., Stolz, J.F., Nord, G.I. Jr., and Phillips, E.J.P. (1987) Anaerobic production of magnetite by a dissimilatory iron-reducing micro-organism. Nature, 330, 252–254.

Lovley, D.R., Coates, J.D., Blunt-Harris, E.L., Phillips, E.J.P., and Woodward, J.C. (1996) Humic substances as electron acceptors for microbial respiration. Nature, 382, 445.

McCammon, C.A., Morrish, A.H., Picone, P.J., and Pollard, R.J. (1986) Site occupancy and aging in hypermagnetite. Journal of Magnetism and Magnetic Materials, 54-57, 1695–1696.

Moskowitz, B.M., Frankel, R.B., Bazylinski, D.A., Jannasch, H.W., and Lovley, D.R. (1989) A comparison of magnetite particles produced anaerobically by magnetotactic and dissimilatory iron-reducing bacteria. Geophysical Research Letters, 16, 665–668.

Murad, E. (1979) Mössbauer and X-ray data on β-FeOOH (akaganeite). Clay Minerals, 14, 273–283.

Nealson, K.H. and Little, B. (1997) Breathing manganese and iron: Solid state respiration. Advances in Applied Microbiology, 45, 213–239.

Roh, Y., Zhang, C.L., Vali, H., Lauf, R.J., Zhou, J., and Phelps, T.J. (2003) Biogeochemical and environmental factors in Fe biomineralization: Magnetite and siderite formation. Clays and Clay Minerals, 51, 83–95.

Scott, D.T., McKnight, D.M., Blunt-Harris, E.L., Kolesar, S.E., and Lovley, D.R. (1998) Quinone moieties act as electron acceptors in the reduction of humic substances by humics-reducing microorganisms. Environmental Science and Technology, 32, 2984.

Sparks, N.H.C., Mann, S., Bazylinski, D.A., Lovley, D.R., Jannasch, H.W., and Frankel, R.B. (1990) Structure and morphology of magnetite anaerobically-produced by a marine magnetotactic bacterium and a dissimilatory iron-reducing bacterium. Earth and Planetary Science Letters, 98, 14–22.

Stookey, L.L. (1970) Ferrozine—A new spectrophotometric reagent for iron. Analytical Chemistry, 42, 779–781.

Tamaura, Y. and Tahata, M. (1990) Complete reduction of carbon dioxide to carbon using cation-excess magnetite. Nature, 346, 255–256.

Tamaura, Y., Akanuma, K., Hasegawa, N., and Tsuji, M. (1994) Synthesis of carbon-iron(II) oxide layer on the surface of magnetite and its reactivity with H_2O for hydrogen generation. Journal of Materials Science, 29, 6175–6180.

Vali, H., Forster, O., Amarantidis, G., and Peterson, N. (1987) Magnetotactic bacteria and their magnetofossils in sediments. Earth and Planetary Science Letters, 86, 389.

van der Zee, C., Roberts, D.R., Rancourt, D.G., and Slomp, C.P. (2003) Nanogoethite is the dominant reactive oxyhydroxide phase in lake and marine sediments. Geology, 31, 993–996.

Wilkin, R.T. and Puls, R.W. (2003) Capstone Report on the Application, Monitoring, and Performance of Permeable Reactive Barriers for Ground-Water Remediation: Volume 1–Performance Evaluations at Two Sites—A report to U.S. EPA. EPA Report: EPA/600/R-03/045a.

Yapp, C.J. (1996) The abundance of $Fe(CO_3)OH$ in goethite and a possible constraint on minimum atmospheric oxygen partial pressures in the Phanerozoic. Geochimica et. Cosmochimica Acta, 60, 4397–4402.

Yapp, C.J. (2004) $Fe(CO_3)OH$ in goethite from a mid-latitude North American oxisol: Estimate of atmospheric CO_2 concentration in the early eocene "climatic optimum". Geochimica et Cosmochimica Acta, 68, 935–947.

Zachara, J.M., Kukkadapu, R.K., Fredrickson, J.K., Gorby, Y.A., and Smith, S.C. (2002) Biomineralization of poorly crystalline Fe^{3+} oxides by dissimilatory metal reducing bacteria (DMRB). Geomicrobiology Journal, 19, 179–207.

MANUSCRIPT RECEIVED MAY 26, 2004
MANUSCRIPT ACCEPTED OCTOBER 13, 2004
MANUSCRIPT HANDLED BY KATRINA EDWARDS